International Journal of Solids and Structures 51 (2014) 1834–1846

Contents lists available at ScienceDirect

International Journal of Solids and Structures

journal homepage: www.elsevier.com/locate/ijsolstr

Discontinuous bifurcation analysis of thermodynamically consistent gradient poroplastic materials

Javier L. Mroginski [a,*], Guillermo Etse [b]

[a] Applied Mechanical Dept., Universidad Nacional del Nordeste, Las Heras 727, Resistencia, Chaco, Argentina
[b] CONICET and Faculty for Exact Sciences & Technology, Universidad Nacional de Tucumán, Maipu 780, 4000 Tucumán, Argentina

ARTICLE INFO

Article history:
Received 12 June 2013
Received in revised form 27 January 2014
Available online 6 February 2014

Keywords:
Gradient theory
Porous media
Localized failure
Softening behavior

ABSTRACT

In this work, analytical and numerical solutions of the condition for discontinuous bifurcation of thermodynamically consistent gradient-based poroplastic materials are obtained and evaluated. The main aim is the analysis of the potentials for localized failure modes in the form of discontinuous bifurcation in partially saturated gradient-based poroplastic materials as well as the dependence of these potentials on the current hydraulic and stress conditions. Also the main differences with the localization conditions of the related local theory for poroplastic materials are evaluated to perfectly understand the regularization capabilities of the non-local gradient-based one. Firstly, the condition for discontinuous bifurcation is formulated from wave propagation analyses in poroplastic media. The material formulation employed in this work for the spectral properties evaluation of the discontinuous bifurcation condition is the thermodynamically consistent, gradient-based modified Cam Clay model for partially saturated porous media previously proposed by the authors. The main and novel feature of this constitutive theory is the inclusion of a gradient internal length of the porous phase which, together with the characteristic length of the solid skeleton, comprehensively defined the non-local characteristics of the represented porous material. After presenting the fundamental equations of the thermodynamically consistent gradient based poroplastic constitutive model, the analytical expressions of the critical hardening/softening modulus for discontinuous bifurcation under both drained and undrained conditions are obtained. As a particular case, the related local constitutive model is also evaluated from the discontinuous bifurcation condition stand point. Then, the localization analysis of the thermodynamically consistent non-local and local poroplastic Cam Clay theories is performed. The results demonstrate, on the one hand and related to the local poroplastic material, the decisive role of the pore pressure and of the volumetric non-associativity degree on the location of the transition point between ductile and brittle failure regimes in the stress space. On the other hand, the results demonstrate as well the regularization capabilities of the non-local gradient-based poroplastic theory, with exception of a particular stress condition which is also evaluated in this work. Finally, it is also shown that, due to dependence of the characteristic lengths for the pore and skeleton phases on the hydraulic and stress conditions, the non-local theory is able to reproduce the strong reduction of failure diffusion that takes place under both, low confinement and low pore pressure of partially saturated porous materials, without loosing, however, the ellipticity of the related differential equations.

1. Introduction

Quasi-brittle materials like soils and concrete have very complex mechanical behaviors when subjected to load histories involving large accumulated inelastic deformations. In these cases, and from the analytical stand point, the evaluation and prediction of the involved failure mode and the location of the transition point between brittle and ductile failure regimes becomes very complex. This is mostly due to the diversity of governing parameters and the variability of their roles in the mechanical degradation processes of these complex materials.

Regarding non-porous continua-based material theories, many authors performed studies to evaluate the post peak behavior and, moreover, the discontinuous bifurcation potentials through the analytical determination of the related critical hardening modulus (see a.o. Zhang et al., 2005; Ottosen and Runesson, 1991;

* Corresponding author. Tel.: +54 3794338418.
E-mail addresses: javierm@ing.unne.edu.ar (J.L. Mroginski), getse@herrera.unt.edu.ar (G. Etse).

http://dx.doi.org/10.1016/j.ijsolstr.2014.01.029
0020-7683/

Runesson et al., 1991, 1996; Perić and Rasheed, 2007). The evaluations covered not only classical local material theories but also anisotropic material formulations (Zhang et al., 2005), as well as constitutive theories related to fiber reinforced materials (Etse et al., 2012; Perić and Rasheed, 2007) and, moreover, to enhanced non-local, gradient-based, materials (Vrech and Etse, 2012).

In case of quasi-brittle porous materials, and due to the diversity and complexity of the involved variables during inelastic degradation process, the discontinuous bifurcation condition was analyzed, so far, by means of different approaches and taking into account the influence of the Lode angle (Zhen et al., 2010), water content or fluid pressure (Liu and Scarpas, 2005), porosity (Zhang et al., 2002), permeability (Zhang and Schrefler, 2001), temperature (Sulem, 2010), etc. Actually, most of the published localization analysis in porous materials (see a.o. Sabatini and Finno, 1996; Benallal and Comi, 2002; Borja, 2004; Ehlers et al., 2004; Kristensson and Ahadi, 2005; Schiava and Etse, 2006), are based on the restrictive consideration that discontinuous bifurcations may only occur in the solid phase. Therefore, and despite the numerous proposals, there is still a need of accurate evaluations of the potentials for discontinuous bifurcation in partially saturated porous materials under more general or arbitrary conditions. This is particularly the case when it comes to assessing the influence of hydraulic and mechanical states of the porous and solid phases, respectively, in the failure modes of partially saturated porous materials, whether brittle or ductile.

Recently, Mroginski et al. (2011), proposed a thermodynamically consistent gradient-based constitutive theory for partially saturated quasi-brittle porous material. It follows the thermodynamic gradient-based formulations for continuous (non-porous) materials by Svedberg and Runesson (1997) and Vrech and Etse (2009), whereby the state variables are the only ones of non-local characters.

The proposal by Mroginski et al. (2011), introduces a novel aspect to more effectively capture the strong influence in failure behaviors of partially saturated porous materials of both the hydraulic and mechanical states of their microstructure. It considers two independent characteristic lengths, for the porous and solid phases, respectively, which are defined in terms of the governed water content and confining pressure. This is in line with the philosophy by Schrefler et al. (2006), in the sense that multiple internal lengths shall be considered to realistically reproduce the strong variation of failure modes of porous material. The capabilities of the thermodynamically consistent gradient-based constitutive theory to predict the variation from localized (brittle) to distributed (ductile) failure modes of quasi-brittle porous materials like soils under different conditions of the water content and confining pressure are demonstrated in Mroginski and Etse (2013).

In this work the discontinuous bifurcation conditions for partially saturated porous materials like soils under both, drained and undrained hydraulic conditions, are numerically and analytically evaluated. The modified Cam Clay model is considered in the framework of the thermodynamically consistent gradient-based formulation by Mroginski et al. (2011).

The numerical study of discontinuous bifurcation condition is based on the identification of the stress domain (under drained and undrained conditions) where the singularity of the localization tensor is fulfilled. On the other hand, the analytical procedure requires the explicit formulation of the critical (minimum) hardening modulus corresponding to the first condition for discontinuous bifurcation in the deformation history of partially saturated porous materials. This is done by means of an extension to the cases of local and gradient-based porous continua of the analytical solutions for discontinuous bifurcation by Ottosen and Runesson (1991), Runesson et al. (1991) and Perić and Rasheed (2007).

After summarizing the most relevant equations of the constitutive theory by Mroginski et al. (2011), this work focuses on formulating its localization tensor and, further, the explicit solutions of the critical hardening modulus for discontinuous bifurcation under both, drained and undrained conditions. The particular cases of plane stress and plain strain are considered.

Then, the potentials for discontinuous bifurcation by means of both the numerical and analytical methods are evaluated for all possible stress states along the first yield surface and the critical state line of both the local and gradient-based Cam-clay constitutive theories for partially saturated poroplastic materials. Drained and undrained hydraulic conditions under both plane strain and plane stress are considered in the analyses.

Regarding the local Cam-clay model for partially saturated porous material the results demonstrates that the position of the transition point for brittle–ductile failure modes in the stress space, and the overall failure mode, do strongly depend on the particular hydraulic and confinement conditions. In this sense, drained hydraulic conditions are more critical for discontinuous bifurcations as well as plane stress conditions.

In case of the gradient-based poroplastic model, the results indicate that its regularization capabilities are able to suppress the discontinuous bifurcation conditions of the local model for all possible stress state, with exception of some particular cases that are evaluated in this work. Nevertheless, and due to the particular form of the gradient characteristic lengths, the non-local model reproduces the increasing degradation of the localization tensor spectral properties as the stress state goes into the small confinement regime and, also, as the pore pressure reduces. In these regimes the non-local model leads to strong reductions of the failure diffusion or quasi-brittle failure modes (minimum eigenvalue of the localization tensor very close to zero). This spectral properties degradation is more critical under drained conditions. Theses results confirm the capabilities of the non-local formulation in this work to reproduce the influence of the stress and hydraulic conditions in the failure modes, in accordance with the experimental evidence on porous media (Vardoulakis, 1996; Sawicki and Świdziński, 2010; Cetin and Gökoĝlu, 2013) and theoretical developments (Runesson et al., 1996; Zhang and Schrefler, 2001; Al Hattamleh et al., 2004).

2. Thermodynamically consistent gradient-based constitutive theory for non-saturated porous media

Porous media are multiphase systems with interstitial voids in the grain matrix filled with water (liquid phase), water vapor and dry air (gas phase) at microscopic level. The mechanical behavior of partially saturated porous media is usually described by the effective stress tensor σ'_{ij}, as follows

$$\sigma'_{ij} = \sigma_{ij} - \delta_{ij} p^w = \sigma^n_{ij} + s_{ij} \quad (1)$$

being σ_{ij} the total stress and $s_{ij} = \delta_{ij}(p^a - p^w)$ and $\sigma^n_{ij} = \sigma_{ij} - \delta_{ij} p^a$ the net and suction stress tensors, respectively, while δ_{ij} is the Kronecker delta. Thereby are p^a and p^w the gas and water pore pressures, respectively. In several geotechnical problems the gas pore pressure can be considered as a constant term that equals the atmospheric pressure. In these cases the suction tensor is counterpart to the water pore pressure, p.

Plastic behavior of quasi-brittle porous materials is related to permanent skeleton strains, but also to permanent variations in fluid mass content, m, due to related porosity variations. To fully characterize current stages of poroplastic media and to describe their inelastic evolutions, the plastic porosity or plastic fluid mass content m^p must be considered in addition to the plastic strain ε^p_{ij}, and to the irreversible entropy density s^p in case of non-isothermal conditions.

Therefore, the poroplastic flow rule is based on additive decompositions of the rates of the dissipative fields into elastic and plastic components

$$\dot{\varepsilon}_{ij} = \dot{\varepsilon}^e_{ij} + \dot{\varepsilon}^p_{ij}; \quad \dot{m} = \dot{m}^e + \dot{m}^p \tag{2}$$

Based on previous works (Svedberg and Runesson, 1997; Vrech and Etse, 2009; Mroginski et al., 2011), the following additive expression of the free energy corresponding to non-local gradient poroplastic materials is adopted

$$\Psi\left(\varepsilon^e_{ij}, m^e, q_\alpha, q_{\alpha,i}\right) = \Psi^e\left(\varepsilon^e_{ij}, m^e\right) + \Psi^{p,loc}(q_\alpha) + \Psi^{p,nloc}(q_{\alpha,i}) \tag{3}$$

where $\Psi^{p,loc}$ and $\Psi^{p,nloc}$ are the local and non-local gradient contributions due to dissipative hardening/softening behaviors, which are expressed in terms of the internal variables q_α and their gradients $q_{\alpha,i}$, respectively, while Ψ^e is the elastic energy of the porous media defined by Coussy (1995) as

$$\Psi^e = \sigma^0_{ij}\varepsilon^e_{ij} + p^0\bar{m}^e + \frac{1}{2}\varepsilon^e_{ij}C^0_{ijkl}\varepsilon^e_{kl} + \frac{1}{2}\mathrm{M}\left(B_{ij}\varepsilon^e_{ij} - \bar{m}^e\right)^2 \tag{4}$$

Thereby are M the Biot's module, $B_{ij} = b\delta_{ij}$ with b the Biot coefficient, $\bar{m}^e = m^e/\rho^{fl}_0$ and $C_{ijkl} = C^0_{ijkl} + MB_{ij}B_{kl}$, with C^0_{ijkl} the fourth-order elastic tensor which linearly relates stress and strain.

The flow rule for general non-associative poroplasticity involves three equations

$$\dot{\varepsilon}^p_{ij} = \dot{\lambda}g^s_{ij}; \quad \dot{m}^p = \dot{\lambda}g^p; \quad \dot{q}_\alpha = \dot{\lambda}g^Q_\alpha \tag{5}$$

being $\Phi(\sigma_{ij}, p, Q_\alpha)$ the convex yield function and $\Phi^*(\sigma_{ij}, p, Q_\alpha)$ the dissipative plastic potential, with Q_α the dissipative stress. Moreover, it is defined $f^s_{ij} = \partial\Phi/\partial\sigma_{ij}$, $g^s_{ij} = \partial\Phi^*/\partial\sigma_{ij}$, $f^p = \partial\Phi/\partial p$, $g^p = \partial\Phi^*/\partial p$, $f^Q_\alpha = \partial\Phi/\partial Q_\alpha$ and $g^Q_\alpha = \partial\Phi^*/\partial Q_\alpha$. Once the Coleman's relations are deduced from the global form of Clausius–Duhem inequality (CDI), while neglecting initial stress and pore pressures, the following rate expressions of the stress tensor $\dot{\sigma}_{ij}$ and pore pressure $\dot{p}$ for drained condition can be obtained

$$\dot{\sigma}_{ij} = C^0_{ijkl}\dot{\varepsilon}_{kl} - B_{ij}\dot{p} - C^0_{ijkl}g^s_{kl}\dot{\lambda} \tag{6}$$

$$\dot{p} = -MB_{ij}\dot{\varepsilon}_{ij} + MB_{ij}\dot{\lambda}g^s_{ij} + M\dot{\bar{m}} - M\dot{\lambda}g^p \tag{7}$$

or, alternatively, for undrained condition

$$\dot{\sigma}_{ij} = C_{ijkl}\dot{\varepsilon}_{kl} - C_{ijkl}\dot{\lambda}g^s_{kl} - MB_{ij}\dot{\bar{m}} + MB_{ij}\dot{\lambda}g^p \tag{8}$$

From the CDI in case of gradient plasticity like the present one follows that the dissipative stress Q_α can be decomposed into its local and non-local components

$$Q_\alpha = Q^{loc}_\alpha + Q^{nloc}_\alpha \tag{9}$$

with

$$Q^{loc}_\alpha = -\rho\partial_{q_\alpha}\Psi \tag{10}$$

$$Q^{nloc}_\alpha = -\left(\rho\partial_{q_{\alpha,i}}\Psi\right)_{,i} \tag{11}$$

A more convenient form of the constitutive equations can be obtained when the plastic multiplier in Eq. (6) and Eq. (8) is replaced by the expression that results from the Kuhn–Tucker conditions,

$$\dot{\lambda} \geqslant 0; \quad \Phi(\sigma_{ij}, p, Q_\alpha) \leqslant 0; \quad \dot{\lambda}\Phi(\sigma_{ij}, p, Q_\alpha) = 0 \tag{12}$$

and the plastic consistency condition

$$\dot{\Phi} = f^s_{ij}\dot{\sigma}_{ij} + f^p\dot{p} + f^Q_\alpha\dot{Q}_\alpha = 0 \tag{13}$$

Eqs. (12) and (13) leads to the following differential expression, from which $\dot{\lambda}$, can be explicitly obtained

$$-\dot{\Phi}^{nloc} + \bar{h}\dot{\lambda} = \dot{\Phi}^e - \dot{\Phi} \tag{14}$$

For more details see Appendix A.

Then, the constitutive expressions of Eqs. (6) and (8) for drained and undrained porous media, respectively, take the form

$$\dot{\sigma}_{ij} = E^{ep,sd}_{ijkl}\dot{\varepsilon}_{kl} + E^{ep,pd}_{ij}\dot{p} - E^{g,spd}_{ij}\dot{f}^g \tag{15}$$

$$\dot{\sigma}_{ij} = E^{ep,su}_{ijkl}\dot{\varepsilon}_{kl} + E^{ep,pu}_{ij}\dot{m}/\rho^{fl}_0 - E^{g,spu}_{ij}\dot{f}^g \tag{16}$$

being $\mathbf{E}^{ep,s}$ and $\mathbf{E}^{ep,p}$ the elastoplastic operators of the solid skeleton and porous phase, respectively, and $\mathbf{E}^{g,sp}$ the continuum gradient-elastoplastic tensor of both constituents. The superscript ^{d} or ^{u} indicates the considered hydraulic condition, drained or undrained, respectively. See Appendix B for more details.

3. Thermodynamically consistent gradient-based modified Cam Clay material model

Originally proposed by Roscoe and Burland (1968) for normally consolidated clays, the modified Cam Clay plasticity model has been extended to a wide range of soils including unsaturated ones (see Alonso et al., 1990; Bolzon et al., 1996), and also to the case of cyclic external actions (see Pedroso and Farias, 2011).

The yield function is defined by

$$\Phi(\sigma', \tau, Q_\alpha) = \left(\sigma' + \frac{\tau^2}{m^2\sigma'}\right) - Q_\alpha \tag{17}$$

where $\sigma' = I_1/3 - p$ is the effective hydrostatic stress, $\tau = \sqrt{3J_2}$ the shear stress, m the Critical State Line (CSL) slope and Q_α the thermodynamically consistent dissipative stress equivalent to the preconsolidation pressure p_{co}. Further, I_1 and J_2 are the first and second invariants of the stress tensor and the deviator tensor, respectively.

Thereby, the following plastic potential is proposed

$$\Phi^*(\sigma', \tau, Q_\alpha) = \eta(\sigma'^2 - \sigma' Q_\alpha) + \left(\frac{\tau}{m}\right)^2 \tag{18}$$

$\eta$is a coefficient that limits the influence of the volumetric pressure during softening regime which is introduced to avoid overestimation of the volumetric compressibility coefficient K_0 in the conventional critical state (see Fig. 1).

The thermodynamic consistency is achieved by assuming the following expression for the dissipative component of the free energy in Eq. (3)

$$\rho\Psi^p\left(\varepsilon^p, \varepsilon^p_{,i}\right) = \rho\Psi^{p,loc}(\varepsilon^p) + \rho\Psi^{p,nloc}\left(\varepsilon^p_{,i}\right) = -\frac{1}{\chi}p^0_{co}\exp(\chi\varepsilon^p) - \left(\frac{1}{2}l^2_\alpha H^{nloc}_\alpha \varepsilon^p_{,i}\right)_{,i} \tag{19}$$

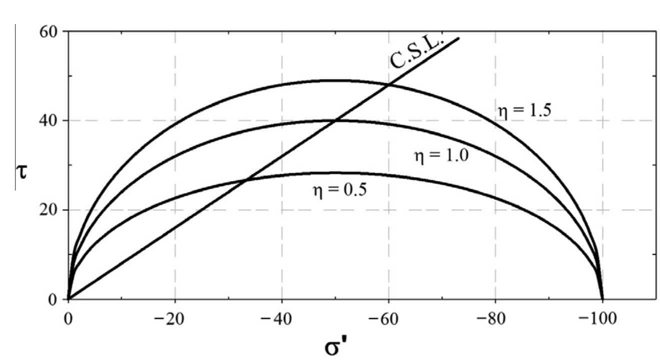

Fig. 1. Modified Cam Clay plasticity model and plastic potential.

being $\chi = -(1+e_0)/(\gamma-\kappa)$, e_0 the initial void ratio, γ a hardening parameter and κ the swelling index (obtained from the Oedometer test). The volumetric plastic strain of the porous media, ε^p, is expressed as a function of the state variables and takes into account the plastic evolutions of the porous and solid phases, in terms of the plastic porosity ϕ^p and the volumetric plastic strain of soil grain ε_s^p (Coussy, 1995)

$$\varepsilon^p = \phi^p + (1-\phi_0)\varepsilon_s^p \tag{20}$$

From Eqs. (10) and (11) the local and non-local dissipative stresses are obtained as follows

$$Q_\alpha^{loc}(\varepsilon^p) = -\rho\partial_{\varepsilon^p}\Psi = p_{co}^0 \exp\left(\chi(\phi^p + (1-\phi_0)\varepsilon_s^p)\right) \tag{21}$$

$$Q_\alpha^{nloc}\left(\varepsilon_{,i}^p\right) = -\rho\left(\partial_{\varepsilon_{,i}^p}\Psi\right)_{,i} = l_s^2 H_s^{nloc}\nabla^2\varepsilon_s^p + l_p^2 H_p^{nloc}\nabla^2\phi^p \tag{22}$$

where l_s and l_p are the internal characteristic lengths for solid skeleton and porous phases, respectively. The numerical implementation of Cam Clay plasticity model in the framework of thermodynamically consistent gradient-based poroplasticity is detailed in Mroginski and Etse (2013).

4. Instability analysis in the form of discontinuous bifurcation

In this section the discontinuous bifurcation analysis for local and non-local thermodynamically consistent porous media is presented.

4.1. Discontinuous bifurcation condition in local porous media

The localization condition in porous media means that either the jump of the velocity gradients

$$[\![\dot{\varepsilon}_{ij}]\!] = 1/2(g_i n_j + n_i g_j) \tag{23}$$

and/or the jump of the rate of fluid mass content

$$[\![\dot{m}]\!] = -[\![M_{i,i}]\!] = -n_i g_i^{\mathrm{M}} \tag{24}$$

is/are different to zero

Applying Hadamard relation (Hadamard, 1903; Coussy, 1995) to the tensors of zero and second orders, p and σ_{ij}, respectively, the following balance equations are obtained

$$\mathrm{c}[\![p_{,i}]\!] + [\![\dot{p}]\!]n_i = 0 \tag{25}$$

$$\mathrm{c}[\![\sigma_{ij,j}]\!] + [\![\dot{\sigma}_{ij}]\!]n_j = 0 \tag{26}$$

being c the discontinuity propagation velocity.

4.1.1. Drained condition

When drained state is considered the instability analysis is restricted to the solid skeleton and the fluid flow in deformable porous media is governed by the Darcy's law.

The fluid subjected to strong pressure gradients may exhibit spontaneous diffusion due to the fluid mass transport. Thereby, the relative flow vector of fluid mass M_i should remain continuous. Thus, form the Darcy's law follows

$$[\![M_i]\!] = -\rho^{fl}k_{ij}[\![p_{,j}]\!] = 0 \tag{27}$$

being k_{ij} the permeability tensor. The last expression implies that the spatial gradients must remain continuous $[\![p_{,i}]\!] = 0$. Thus, from Eq. (25) follows that the rate of pore pressure must remain continuous as well, i.e. $[\![\dot{p}]\!] = 0$.

Considering the momentum balance equation for quasi-static problems, applying the jump operator to the incremental constitutive equation, Eq. (15), and substituting the resulting expression into Eq. (26), we obtain

$$[\![\dot{\sigma}_{ij}]\!]n_j = E_{ijkl}^{ep,sd}[\![\dot{\varepsilon}_{kl}]\!]n_j = 0 \tag{28}$$

being $E_{ijkl}^{ep,sd}$ the solid skeleton elastoplastic tensor, as described in Section 3. Introducing Eq. (23) in Eq. (28) results

$$[\![\dot{\sigma}_{ij}]\!]n_j = A_{ij}^{d,loc}g_j = 0 \tag{29}$$

where the elastoplastic acoustic tensor for local poroplasticity under drained condition can be decomposed in its elastic, $A_{ij}^{d,e,s}$, and elastoplastic parts, $A_{ij}^{d,ep,s}$, as

$$A_{ij}^{d,loc} = E_{ijkl}^{ep,sd}n_l n_k = A_{ij}^{d,e,s} - A_{ij}^{d,ep,s} \tag{30}$$

being

$$A_{ij}^{d,e,s} = C_{ijkl}^0 n_l n_k \qquad A_{ij}^{d,ep,s} = \frac{C_{ijmn}^0 g_{mn}^s f_{pq}^s C_{pqkl}^0}{\bar{h}} n_l n_k \tag{31}$$

and $\bar{h}$ the generalized plastic modulus defined in Appendix A. Non-trivial solutions of Eq. (29) can be obtained from the spectral analysis of the local poroplastic acoustic tensor $A_{ij}^{d,loc}$. Then, the localization condition of drained porous media is achieved as

$$\det\left(A_{ij}^{d,loc}\right) = 0 \tag{32}$$

Consequently, the localization tensor in fully drained condition takes the same form as in classical elastoplastic continua. It should be noted that, since the localization condition in Eq. (32) involves only the drained poroelastic properties, the influence of the fluid pressure in the localization condition is taken into account through its influence on the loading function Φ and the generalized plastic modulus h.

4.1.2. Undrained state

In undrained conditions the variation of fluid mass content in the solid skeleton vanishes, $\dot{m} = 0$. The pore pressure can be obtained from the solid skeleton kinematics, $g_i \equiv g_i^{\mathrm{M}}$. Then, from the constitutive expression of Eq. (16) and the jump of the velocity gradients Eq. (23), follows

$$[\![\dot{\sigma}_{ij}]\!]n_j = A_{ij}^{u,loc}g_j = 0 \tag{33}$$

where, similarly to the previous section, the elastoplastic acoustic tensor for local poroplasticity under undrained condition can be decomposed in the elastic and plastic components of both the solid and porous phases, as well as the coupled elastoplastic acoustic tensor for solid and porous phases, $A_{ij}^{u,ep,sp}$, as

$$A_{ij}^{u,loc} = E_{ijkl}^{ep,su}n_l n_k = A_{ij}^{u,e,s} + A_{ij}^{u,e,p} - A_{ij}^{u,ep,s} - A_{ij}^{u,ep,p} + A_{ij}^{u,ep,sp} \tag{34}$$

being

$$\begin{aligned} A_{ij}^{u,e,s} &= C_{ijkl}^0 n_l n_k \\ A_{ij}^{u,e,p} &= \mathrm{M}B_{ij}B_{kl}n_l n_k \\ A_{ij}^{u,ep,s} &= \frac{C_{ijmn}g_{mn}^s f_{pq}^s C_{pqkl}}{\bar{h}} n_l n_k \\ A_{ij}^{u,ep,p} &= \mathrm{M}^2\frac{g^p B_{ij}B_{kl}f^p}{\bar{h}} n_l n_k \\ A_{ij}^{u,ep,sp} &= \mathrm{M}\left(\frac{C_{ijmn}g_{mn}^s B_{kl}f^p}{\bar{h}} + \frac{g^p B_{ij}C_{klmn}f_{mn}^s}{\bar{h}}\right)n_l n_k \end{aligned} \tag{35}$$

The localization condition follows from the spectral analysis of the acoustic tensor

$$\det\left(A_{ij}^{u,loc}\right) = 0 \tag{36}$$

From the comparison between Eq. (32) and Eq. (36) and, moreover, of Eq. (30) and Eq. (34), it can be concluded that the hydraulic conditions strongly affect the localization indicator performance.

4.2. Bifurcation analysis in gradient-based poroplastic media

In previous section the discontinuous bifurcation problem of local porous medium has been studied.

In the following the occurrence of localized failure modes in the form of discontinuous bifurcation is analyzed in case of gradient elastoplastic porous media. Homogeneous fields of stress and strain rates just before the onset of localization are assumed. Contrarily to the case of local poroplasticity, the plastic consistency, see Eq. (14), is now a function of both the plastic multiplier $\dot{\lambda}$ and its second order gradient $\dot{\lambda}_{,ij}$.

The loss of ellipticity of constitutive equations is commonly investigated by means of a wave propagation analysis (Abellan and de Borst, 2006; Tsagrakis et al., 2003; Benallal and Comi, 2002; Liebe et al., 2001; Svedberg and Runesson, 1997). Thus, the following harmonic perturbations to the incremental field variables, i.e. displacements, mass content and plastic multiplier are applied, representing the propagation of stationary planar waves

$$\begin{bmatrix} \dot{u}(\boldsymbol{x},t) \\ \dot{\gamma}(\boldsymbol{x},t) \\ \dot{\lambda}(\boldsymbol{x},t) \end{bmatrix} = \begin{bmatrix} \dot{\mathcal{U}}(t) \\ \dot{\mathcal{M}}(t) \\ \dot{\mathcal{L}}(t) \end{bmatrix} \exp\left(\frac{i2\pi}{\delta}\boldsymbol{n}\cdot\boldsymbol{x}\right) \tag{37}$$

being $\dot{\gamma}$ the mass content, $\boldsymbol{x}$ the position vector (in Cartesian coordinates), $\boldsymbol{n}$ the wave normal direction and δ the wave length. Moreover $\dot{\mathcal{U}}$, $\dot{\mathcal{M}}$ and $\dot{\mathcal{L}}$ are the wave solutions, when they are homogeneously distributed in the space.

Applying the equilibrium condition on the discontinuity surface and replacing Eqs. (37) in the plastic consistency condition for gradient plasticity Eq. (14), while considering Eq. (6) or Eq. (8) results

$$\left(\frac{2\pi}{\delta}\right)^2 \left\{ C^0_{ijkl} - \frac{C^0_{ijmn} g^s_{mn} f^s_{pq} C^0_{pqkl}}{\bar{h} + \bar{h}^{nloc}} \right\} n_l n_k\, \dot{\mathcal{U}} = 0 \tag{38}$$

for drained conditions, and

$$\left(\frac{2\pi}{\delta}\right)^2 \left\{ C^0_{ijkl} + \mathrm{M} B_{ij} B_{kl} - \frac{C_{ijmn} g^s_{mn} f^s_{pq} C_{pqkl}}{\bar{h} + \bar{h}^{nloc}} - \mathrm{M}^2 \frac{g^p B_{ij} B_{kl} f^p}{\bar{h} + \bar{h}^{nloc}} + \mathrm{M}\left(\frac{C_{ijmn} g^s_{mn} B_{kl} f^p}{\bar{h} + \bar{h}^{nloc}} + \frac{g^p B_{ij} C_{mnkl} f^s_{mn}}{\bar{h} + \bar{h}^{nloc}} \right) \right\} n_l n_k\, \dot{\mathcal{U}} = 0 \tag{39}$$

for undrained conditions, being $\bar{h}^{nloc}$ the generalized gradient modulus

$$\bar{h}^{nloc} = l^2_\alpha \left(f^Q_\alpha g^Q_\alpha H^{nloc}_{\alpha ij} \right) n_j n_i \left(\frac{2\pi}{\delta}\right)^2 \tag{40}$$

The expressions between brackets in Eqs. (38) and (39) are the acoustic tensors for non-local gradient plasticity under drained and undrained conditions, respectively. Following the nomenclature of Eqs. (30) and (34), these tensors can be decomposed as follows

$$A^{d,nloc}_{ij} = A^{d,e,s}_{ij} - A^{d,gr,s}_{ij} \tag{41}$$

$$A^{u,nloc}_{ij} = A^{u,e,s}_{ij} + A^{u,e,p}_{ij} - A^{u,gr,s}_{ij} - A^{u,gr,p}_{ij} + A^{u,gr,sp}_{ij} \tag{42}$$

From the comparison between the localization tensors of local porous media, Eqs. (31) and (35), and those to non-local gradient continua, Eqs. (38) and (39), follows that the difference lies only in the generalized gradient modulus $\bar{h}^{nloc}$. The effects of $\bar{h}^{nloc}$ are, at the constitutive level, the well posedness of the involved differential equations and, at the FE level, the regularization of the post-peak behavior.

5. Spectral analysis for discontinuous bifurcation

Since the existence of discontinuous bifurcation requires the singularity of the acoustic tensor deduced above, its eigenvalue problem plays a very important role. In this work analytical solutions of the acoustic tensor's eigenvalue problem are obtained by extending the procedure proposed by Ottosen and Runesson (1991) and Perić (1990) for the cases of local and gradient-based partially saturated porous materials. This analytical method leads to explicit solutions of the critical hardening modulus (local and non-local), H_{crit}, for the onset of localization.

The eigenvalue analysis is firstly performed for the undrained acoustic tensor of the gradient poroplastic material. Then, the explicit solution of the critical hardening modulus for discontinuous bifurcation of the local poroplastic material under undrained condition is obtained as a particular case.

It should be noted that in the non-local material, when the Biot modulus M tends to zero the tensor $A^{u,nloc}_{ij}$ approaches $A^{d,nloc}_{ij}$, while the critical hardening modulus for drained gradient-poroplasticity takes a very similar form to those deduced for gradient non-porous media (Vrech and Etse, 2012). That it is why the drained condition will not be considered in this section.

The classical eigenvalue problem may be written as

$$\left(Q_{ij} - \delta_{ij}\lambda^{(i)} \right) y^{(i)} = 0 \tag{43}$$

being $\lambda^{(i)}$ and $y^{(i)}$ the eigenvalues and eigenvectors, respectively, and Q_{ij}:

$$Q_{ij} = \delta_{ij} - \frac{1}{\bar{h} + \bar{h}^{nloc}} \left(P^e_{ik} b^s_k a^s_j + \mathrm{M}^2 P^e_{ik} b^p_k a^p_j - \mathrm{M} P^e_{ik} \left(b^s_k a^p_j + b^p_k a^s_j \right) \right) \tag{44}$$

with

$$\begin{aligned} b^s_j &= n_i C_{ijkl} g^s_{kl} \\ a^s_k &= f^s_{ij} C_{ijkl} n_l \\ b^p_j &= n_i B_{ij} g^p \\ a^p_j &= f^p B_{kl} n_l \\ P^e_{ik} &= \left(A^{u,e,s}_{ij} + A^{u,e,p}_{ij} \right)^{-1} \end{aligned} \tag{45}$$

It should be noted that the tensor P^e_{ik} is the inverse of the elastic acoustic tensor for gradient porous media. The matrix $P^e_{ik} b_k a_j$ can be written as $p_i a_j$, where $p_i = P^e_{ik} b_k$. Therefore, the actual rank of Q_{ij} is one. Then, $\lambda^{(1)} = \lambda^{(2)} = 1$, and the remaining eigenvalue can be obtained from the condition $Q_{jj} = \lambda^{(1)} + \lambda^{(2)} + \lambda^{(3)} = 2 + \lambda^{(3)}$, as

$$\lambda^{(3)} = 1 - \frac{1}{\bar{h} + \bar{h}^{nloc}} \left(P^e_{ik} b^s_k a^s_j + \mathrm{M}^2 P^e_{ik} b^p_k a^p_j - \mathrm{M} P^e_{ik} \left(b^s_k a^p_j + b^p_k a^s_j \right) \right) \tag{46}$$

Non trivial solutions of Eq. (43) are obtained when the minimum eigenvalue $\lambda^{(3)} = 0$. From Eqs. (45) and (46) follows the hardening modulus

$$\bar{H}_{crit} = \bar{H} + \bar{h}^{nloc} = P^e_{ik} b^s_k a^s_j + \mathrm{M}^2 P^e_{ik} b^p_k a^p_j - \mathrm{M} P^e_{ik} \left(b^s_k a^p_j + b^p_k a^s_j \right) - f^s_{ij} C_{ijkl} g^s_{kl} + \mathrm{M}\left(f^s_{ij} B_{ij} g^p + f^p B_{ij} g^s_{ij} - f^p g^p \right) \tag{47}$$

Assuming elastic isotropy of the solid phase C^0_{ijkl}, and considering $C_{ijkl} = C^0_{ijkl} + \mathrm{M} B_{ij} B_{kl}$, then the elastic stiffness tensor for poroelastic media results

$$C_{ijkl} = G\left(\delta_{ik}\delta_{jl} + \delta_{il}\delta_{jk} \right) + \omega \delta_{ij}\delta_{kl} \tag{48}$$

where G is the shear modulus, ν the Poisson ratio and $\omega = 2G\nu/\ (1 - 2\nu) + \mathrm{M}b^2$. The elastic acoustic tensor for gradient poroplasticity $A^{u,e}_{ij} = A^{u,e,s}_{ij} + A^{u,e,p}_{ij}$ in Eq. (42) and its inverse P^e_{ij} become

$$A^{u,e}_{ij} = G(\gamma n_i n_j + \delta_{ij}); \quad P^e_{ij} = \frac{1}{G}(-\phi n_i n_j + \delta_{ij}) \tag{49}$$

being $\phi = \left[G + \mathrm{M}b^2(1 - 2\nu) \right] \left[2G(1 - \nu) + \mathrm{M}b^2(1 - 2\nu) \right]^{-1}$ and $\gamma = \ 1/(1 - 2\nu) + \mathrm{M}b^2/G$. With these expressions the hardening modulus given by Eq. (47) takes the form

$$\bar{H}_{crit} = 4G\phi n_i f^s_{ij} n_j n_k g^s_{kl} n_l + f^s_{ii} g^s_{ii}\left[\frac{\omega^2}{G}(1-\phi)-\omega\right] + 4Gn_i f^s_{ij} g^s_{jk} n_k - 2Gf^s_{ij} g^s_{ij} + 2\omega(1-\phi)n_i\left(g^s_{kk} f^s_{ij} + f^s_{kk} g^s_{ij}\right)n_j - 2\mathrm{M}b(1-\phi)n_i\left(g^p f^s_{ij} + f^p g^s_{ij}\right)n_j + \left(g^p f^s_{ii} + f^p g^s_{ii}\right)\left[\mathrm{M}b - \frac{\mathrm{M}b\omega}{G}(1-\phi)\right] + f^p g^p\left[\frac{\mathrm{M}^2 b^2}{G}(1-\phi) - \mathrm{M}\right] \quad (50)$$

A more convenient expression could be obtained considering the decomposition of f^s_{ij} and g^s_{ij} into their deviatoric and volumetric parts

$$\bar{f}^s_{ij} = f^s_{ij} - \frac{1}{3}\delta_{ij} f^s; \quad \bar{g}^s_{ij} = g^s_{ij} - \frac{1}{3}\delta_{ij} g^s \quad (51)$$

where $\bar{f}^s_{ij}$ and f^s denote the deviatoric and volumetric parts of f^s_{ij}, while $\bar{g}^s_{ij}$ and g^s those of g^s_{ij}, respectively.

With this notation Eq. (50) can be rewritten as

$$\frac{\bar{H}_{crit}}{4G} = -\frac{1}{2}\bar{f}^s_{ij}\bar{g}^s_{ij} - \alpha_0 n_i \bar{f}^s_{ij} n_j n_k \bar{g}^s_{kl} n_l + \alpha_1 f^s g^s + n_i\left(\alpha_2 g^s \bar{f}^s_{ij} + \alpha_2 f^s \bar{g}^s_{ij} + \bar{g}^s_{ij}\bar{f}^s_{ij}\right)n_j + \alpha_3 n_i\left(g^p \bar{f}^s_{ij} + f^p \bar{g}^s_{ij}\right)n_j + \alpha_4(f^p g^s + g^p f^s) + \alpha_5 f^p g^p \quad (52)$$

being

$$\begin{aligned} \alpha_0 &= \phi \\ \alpha_1 &= \frac{\omega(1-\phi)}{G}\left(\frac{1}{3} + \frac{\omega}{4G}\right) - \left(\frac{\omega}{4G} + \frac{\phi}{9} + \frac{1}{18}\right) \\ \alpha_2 &= \frac{1-\phi}{3} + \frac{\omega(1-\phi)}{2G} \\ \alpha_3 &= \frac{\mathrm{M}b(1-\phi)}{2G} \\ \alpha_4 &= \frac{\mathrm{M}b}{4G}\left[1-(1-\phi)\frac{\omega}{G}\right] - \frac{\mathrm{M}b(1-\phi)}{6G} \\ \alpha_5 &= (1-\phi)\left(\frac{\mathrm{M}b}{2G}\right)^2 - \frac{\mathrm{M}}{4G} \end{aligned} \quad (53)$$

The particular case of identical principal directions for f^s_{ij} and g^s_{ij} is considered

$$\bar{f}^s_{ij} = \begin{bmatrix} \bar{f}^s_1 & 0 & 0 \\ 0 & \bar{f}^s_2 & 0 \\ 0 & 0 & \bar{f}^s_3 \end{bmatrix}; \quad \bar{g}^s_{ij} = \begin{bmatrix} \bar{g}^s_1 & 0 & 0 \\ 0 & \bar{g}^s_2 & 0 \\ 0 & 0 & \bar{g}^s_3 \end{bmatrix} \quad (54)$$

being $\bar{f}^s_1 \geqslant \bar{f}^s_2 \geqslant \bar{f}^s_3$ and $\bar{g}^s_1 \geqslant \bar{g}^s_2 \geqslant \bar{g}^s_3$ their principal values.

Moreover, in cohesive-frictional material like soils, a volumetric non-associative flow rule can be considered, i.e. $\bar{f}^s_i = \bar{g}^s_i$ and $f^s \neq g^s$.

With these assumptions Eq. (52) becomes

$$\frac{\bar{H}_{crit}}{4G} = -\alpha_0\left(\bar{f}^s_i n_i^2\right)^2 + \left(r\bar{f}^s_i + \left(\bar{f}^s_i\right)^2\right)n_i^2 + \alpha_4(f^p g^s + g^p f^s) + k \quad (55)$$

being $r = \alpha_2(f^s + g^s) - \alpha_3(f^p + g^p)$ and $k = -\frac{1}{2}\left(\bar{f}^s_i\right)^2 + \alpha_1 f^s g^s + \alpha_5 f^p g^p$.

Using the Lagrange multiplier method the maximum condition or critical value $\bar{H}_{crit}$ can be evaluated

$$\mathcal{L} = \frac{\bar{H}_{crit}}{4G} - \ell\left(n_1^2 + n_2^2 + n_3^2 - 1\right) \quad (56)$$

where ℓ is the Lagrangian multiplier. It appears that the critical hardening modulus and its critical direction are highly dependent on two coefficients, r and c_{13} or c_{31}.

$$c_{13} = \bar{f}^s_1 + (1-2\alpha_0)\bar{f}^s_3 + r; \quad c_{31} = \bar{f}^s_3 + (1-2\alpha_0)\bar{f}^s_1 + r \quad (57)$$

Then, the critical hardening modulus can be obtained by

$$r \leqslant 0 \begin{cases} \bar{H}_{crit} = \frac{G}{\alpha_0}\left(\bar{f}^s_1 + \bar{f}^s_3 + r\right)^2 - \bar{f}^s_1\bar{f}^s_3 + c; & \text{for } c_{13} \geqslant 0 \\ \bar{H}_{crit} = 4G(1-\alpha_0)\bar{f}^{s2}_3 + r\bar{f}^s_3 + c; & \text{for } c_{13} \leqslant 0 \end{cases} \quad (58)$$

$$r \geqslant 0 \begin{cases} \bar{H}_{crit} = \frac{G}{\alpha_0}\left(\bar{f}^s_1 + \bar{f}^s_3 + r\right)^2 - \bar{f}^s_1\bar{f}^s_3 + c; & \text{for } c_{31} \leqslant 0 \\ \bar{H}_{crit} = 4G(1-\alpha_0)\bar{f}^{s2}_1 + r\bar{f}^s_1 + c; & \text{for } c_{31} \geqslant 0 \end{cases} \quad (59)$$

with $c = \alpha_4(f^p g^s + f^s g^p) + k$.

The critical directions for localization are summarized in Table 1. Two cases were considered: $r \geqslant 0$ and $r \leqslant 0$, being $\rho = 2\alpha_0(\bar{f}^s_1 - \bar{f}^s_3)$.

Finally, the special case $\bar{f}^s_1 = \bar{f}^s_2 = \bar{f}^s_3 = 0$ is considered. In this trivial situation the critical hardening modulus remains constant

$$\bar{H}_{crit} = 4Gc \quad (60)$$

5.1. Limiting cases of gradient plasticity regularization capabilities

In this section, the limitations signalized in Vrech and Etse (2006, 2012) of gradient plasticity regularization capabilities are evaluated. Two particular cases are considered as follow:

Case 1: The wave length $\delta \to \infty$, then $\bar{h}^{nloc} \to 0$ (from Eq. (40)) and $\bar{H}_{crit} \to \bar{H}$, i.e. the local poroplasticity case is recovered.

Case 2: The local hardening modulus satisfies the condition $\bar{H} < \bar{H}_{crit}$ and, therefore, the critical non-local modulus results $\bar{h}^{nloc}_{crit} = \bar{H}_{crit} - \bar{H}$. Thus, if the adopted non-local hardening modulus is smaller than the critical one, i.e. $\bar{h}^{nloc} < \bar{h}^{nloc}_{crit}$, then the regularization capabilities of the non-local gradient-based poroplastic theory by Mroginski et al. (2011) are suppressed. With other words, in this case 2, localized failure mode in the form of discontinuous bifurcation takes place despite the gradient-based constitutive formulation.

6. Localization analysis of modified Cam Clay poroplastic material

In this section the spectral properties of the acoustic tensors for local and gradient modified Cam Clay poroplastic materials under plane strain and plane stress conditions are analyzed. Several numerical examples are taken into account to evaluate the failure modes of the considered local and non-local porous materials in drained and undrained conditions.

The material properties used in the following analysis are summarized in Table 2.

Following the procedure in Section 5 the critical hardening modulus of the local and non-local modified Cam Clay poroplastic model is evaluated considering undrained conditions. Three different equilibrium stress states on the initial yield surface are considered, see Fig. 2.

The variation of the hardening modulus with the inclination angle of the normal direction to the potential discontinuity surface, for each one of the three considered stress states are plotted in Fig. 3, both for the local and non-local materials. Also the critical hardening modulus for each stress state as predicted following the analytical approach in Section 5 is depicted with a circle on each curve in Fig. 3. It can be observed that the local model leads to null value of the critical hardening modulus in case of the stress state associated with the lowest confining pressure. In the other two stress states with larger confinement, the critical hardening modulus is negative, indicating that the discontinuous bifurcation takes place in the post-peak regime. The non-local model leads to negative values of the critical hardening modulus in all three stress states, indicating that the critical condition for localization, even in case of the smallest confinement, does not take place in pre-peak

Table 1
Critical directions for $\bar{H}_{crit}$.

	$r \leqslant 0$		$r \geqslant 0$	
	$c_{13} \geqslant 0$	$c_{13} < 0$	$c_{31} \leqslant 0$	$c_{31} > 0$
$\bar{f}_1^s > \bar{f}_2^s > \bar{f}_3^s$	$n_1^2 = c_{13}/\rho$ $n_2^2 = 0$ $n_3^2 = -c_{31}/\rho$	$n_1^2 = 0$ $n_2^2 = 0$ $n_3^2 = 1$	$n_1^2 = c_{31}/\rho$ $n_2^2 = 0$ $n_3^2 = -c_{31}/\rho$	$n_1^2 = 1$ $n_2^2 = 0$ $n_3^2 = 0$
$\bar{f}_1^s = \bar{f}_2^s > \bar{f}_3^s$	$n_1^2 + n_2^2 = c_{13}/\rho$ $n_3^2 = -c_{31}/\rho$	$n_1^2 = n_2^2 = 0$ $n_3^2 = 1$	$n_1^2 + n_2^2 = c_{13}/\rho$ $n_3^2 = -c_{31}/\rho$	$n_1^2 + n_2^2 = 1$ $n_3^2 = 0$
$\bar{f}_1^s > \bar{f}_2^s = \bar{f}_3^s$	$n_1^2 = c_{13}/\rho$ $n_2^2 + n_3^2 = -c_{31}/\rho$	$n_1^2 = 0$ $n_2^2 + n_3^2 = 1$	$n_1^2 = c_{13}/\rho$ $n_2^2 + n_3^2 = -c_{31}/\rho$	$n_1^2 = 1$ $n_2^2 = n_3^2 = 0$

Table 2
Soil material parameters.

Material parameters	Value
CSL slope, m	0.856
Preconsolidation pressure, p_{co}	100.00 Mpa
Initial pore pressure, p	−10.00 Mpa
Initial porosity, ϕ_0	0.4
Bulk compressibility coefficient, K_0	1000.00
Solid compressibility coefficient, K_s	1500.00
Fluid compressibility coefficient, K_{fl}	1000.00
Biot coefficient, $b = 1 - K_0/K_s$	0.33
Biot module inverse, $M1 = M^{-1} = (b - \phi_0)/K_s + \phi_0/K_f$	$3.56 * 10^{-4}$
Young module, E	20000.0 Mpa
Poisson ratio, ν	0.2
Non-associativity coefficient η (from Eq. (18))	0.15

regime. Moreover, in all three stress states the critical hardening module is smaller than that corresponding to the local model, indicating that the gradient-based formulation delays the occurrence of discontinuous bifurcations in comparison to the local model. Finally, it can be observed that the negativity of the critical hardening modulus of the non-local model strongly decreases with the reduction of the confining pressure. In case of the stress state with the lowest confinement, the critical hardening modulus of the non-local model turns very close to zero, while still negative. This demonstrates that the gradient-based formulation considered in this work is able to reproduce quasi-brittle failure forms in case of stress states in the low confinement regime while suppressing the occurrence of discontinuous bifurcation condition in the pre-peak regime.

Following, the evaluation of the critical hardening modulus of the local model is performed along the entire failure surface in the principal stress space, σ_1 and σ_2. The particular case of plane strain whereby $\sigma_3 = \nu(\sigma_1 + \sigma_2)$ is considered in the evaluations

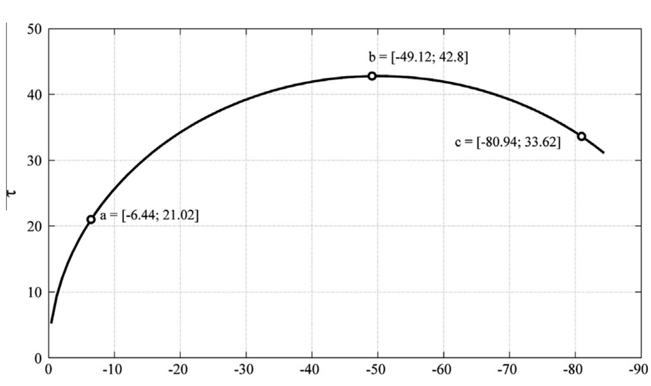

Fig. 2. Considered stress states.

shown in Fig. 4. On the other hand, in Fig. 5 the same analysis is carried out considering plane stress condition, i.e. $\sigma_3 = 0$.

The results in Figs. 4 and 5 demonstrate that the local modified Cam Clay model signalizes discontinuous bifurcation in the pre-peak regimes of stress paths in the low confinement region both in drained and undrained conditions. It can be concluded that the drained condition is more critical for localization than the undrained one, while the combination between plane stress state and drained condition, is the most critical one.

Next, the spectral properties of the acoustic localization tensor for non-local gradient poroplastic Cam Clay model are further evaluated. The material properties presented in Table 2 are considered. The performance of the acoustic tensor determinant for drained conditions in both classical and gradients plasticity for plane strain conditions are presented in Fig. 6. Positive values of the determinant of the acoustic tensor are plotted with outside normal vectors. This representation allows a clear identification of the initial yield surface region where discontinuous bifurcation takes place and of the location of the transition point (TP) between brittle and ductile failure (indicated with a circle in Fig. 6). The Cam Clay gradient-plasticity formulation suppresses the localized failure modes with exception of a very limited zone of the initial yield surface under drained condition and for very low confinement. In this zone the localization indicator approaches zero but remains positive. The results in Fig. 6 demonstrate that the non-local material model, due to the particular form the gradient characteristic length is defined, is able to reproduce the reduction of the failure diffusion (and failure ductility) that occurs in porous materials, when the stress states moves along the initial yield surface under decreasing confinement. Nevertheless, the well-posedness of the differential equations and, therefore, the objectivity of the associated FE solution are achieved along the entire yield surface. Contrarily, the local model is much more critical for localized failure modes and discontinuous bifurcations. Moreover, the TP in the drained case takes place at higher confinement than in the undrained one.

The discontinuous bifurcation evaluation along the first yield surface corresponding to the most critical case for localized failure, i.e. the drained condition under plane stress state, is presented in Fig. 7. As can be observed, when it comes to the local model, the localized failure regime covers a very important sector of the initial yield surface, while it strongly reduces in case of the gradient-based model. In the last case, however, the localization tensor remains positive defined.

In the next, the influences of the pore water pressure and of the non-associativity degree on the localized failure indicator are evaluated in the spaces (σ', det(A), p) and (σ', det(A), η), respectively.

Firstly, Figs. 8 and 9 show, for drained and undrained conditions, respectively, the performance of the localization indicator along the initial yield surface of the local model under plane strain conditions. Similarly, Figs. 10 and 11 illustrate the influence of the pore pressure on the localization indicator for local poroplasticity

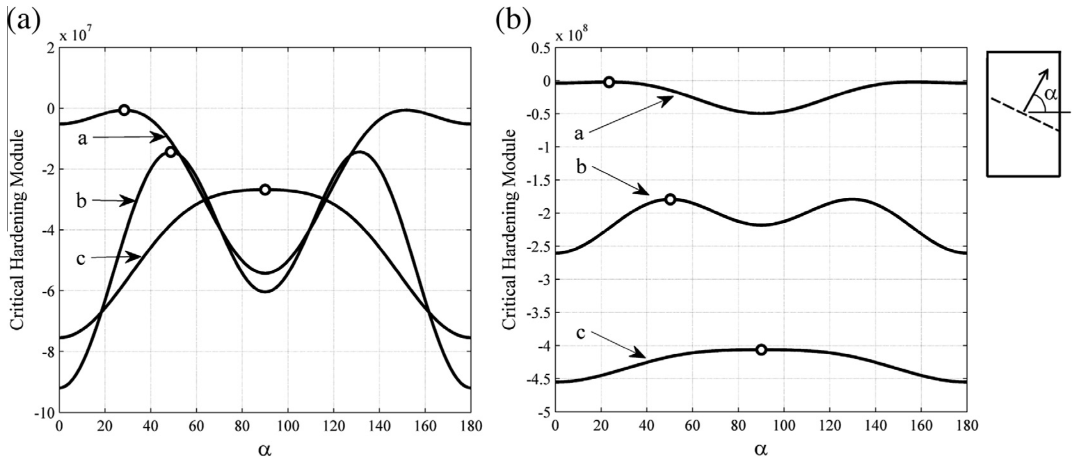

Fig. 3. Critical hardening modulus prediction of the stress states pointed out in Fig. 2 considering undrained condition for: (a) local poroplasticity; (b) non-local gradient poroplasticity.

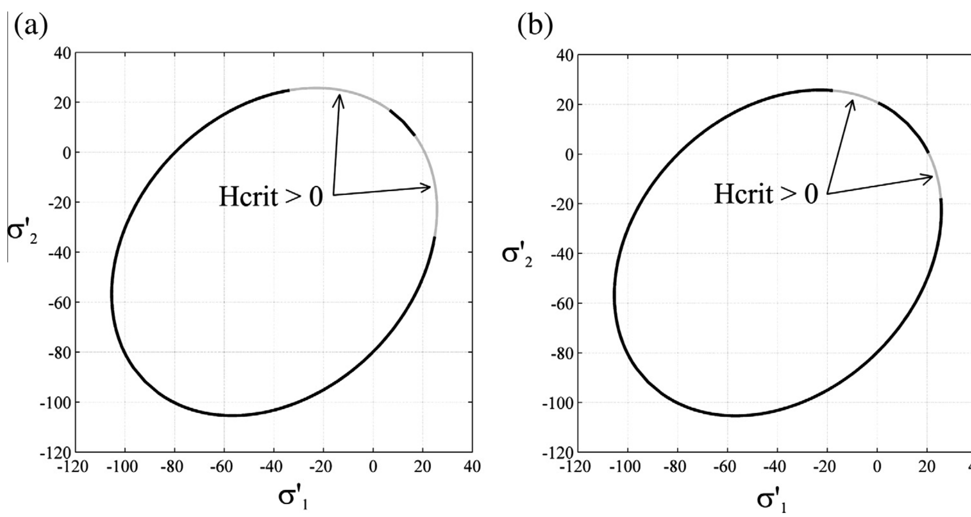

Fig. 4. Critical hardening modulus along initial yield surface in principal stress space and assuming plain strain state, for: (a) drained condition; (b) undrained condition.

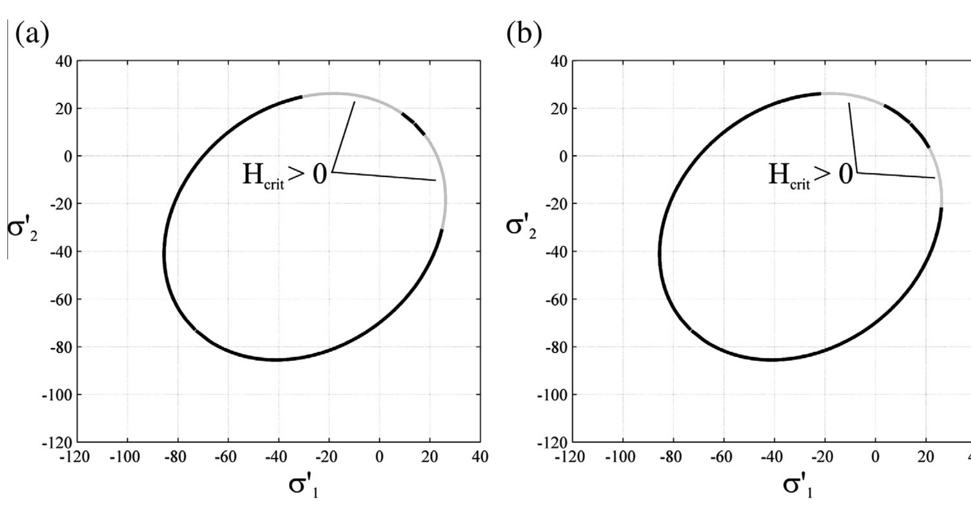

Fig. 5. Critical hardening modulus along initial yield surface in principal stress space and assuming plain stress state, for: (a) drained condition; (b) undrained condition.

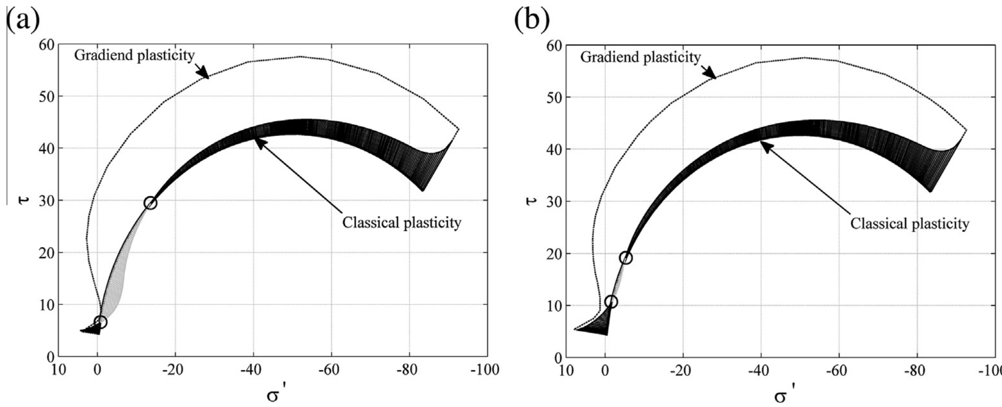

Fig. 6. Localization condition on the initial yield surface for: (a) drained condition; (b) undrained condition, assuming plain strain state.

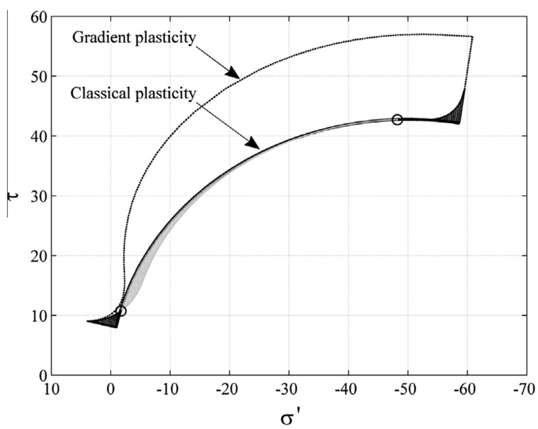

Fig. 7. Localization condition for drained hydraulic condition on the initial yield surface, assuming plain stress state.

under plane stress conditions, and for the drained and undrained cases, respectively.

It can be clearly recognized the strong influence of the pore pressure p and of the hydraulic condition in the failure mode of the local modified Cam Clay model. Under drained condition, localized failure modes occur in a large portion of the stress-pore pressure space. Contrarily, the undrained case is associated with more stable failure behaviors. From Figs. 12 and 13, it can be observed that the non-local modified Cam Clay model leads to diffuse failure modes (positive values of the localization indicator) for the entire considered stress-pore pressure space of the initial yield surface when both drained and undrained conditions as well as plain strain and plain stress states are considered. Nevertheless, and as said before, due to the form the characteristic length is defined, this material model is able to reproduce the increasing reduction of the failure diffusion (reduction of the localization tensor positiveness) that takes place under decreasing confinement and pore pressure. This is in agreement with failure behaviors experimentally observed in partially saturated porous materials like soils.

Finally, the influence of the non-associativity of the local and non-local Cam Clay materials in the discontinuous bifurcation condition is analyzed. Fig. 14 shows the results corresponding to the local and non-local models, under both drained and undrained conditions, in case of plain strain. Fig. 15 shows same results in case of plain stress. As can be observed in these results, the non-associativity degree which represents the plastic volumetric dilatation, strongly destabilizes the failure mode of porous frictional materials. However, the influence of the non-associativity degree on the failure mode is considerably more relevant in the local material, for all different considered cases. Moreover, in the non-local porous material, the failure mode destabilization is limited to extremely (and unrealistically) small values of the volumetric non-associativity degree.

In Fig. 16, the regularization limitation of the gradient-based poroplastic theory in this work as detailed in case 2 of Section 5.1 is evaluated. Constant value of the initial pore pressure equal to -10 kPa is considered under both plane strain and plane stress states.

Finally, in Fig. 17, a large spectrum of possible pore pressure, from 0 to -50 kPa is considered in the evaluation of the regularization limitations of the gradient poroplastic theory. The results

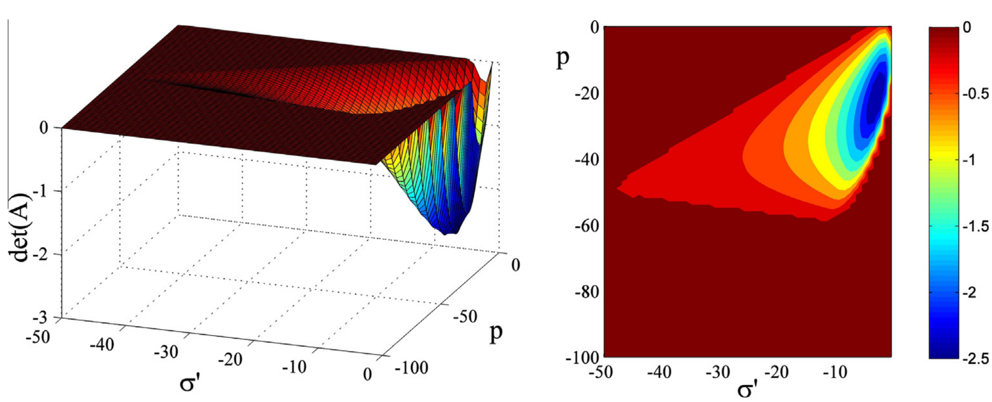

Fig. 8. Discontinuous bifurcation condition in (σ', det(A), p) space for drained condition assuming plain strain state and local plasticity.

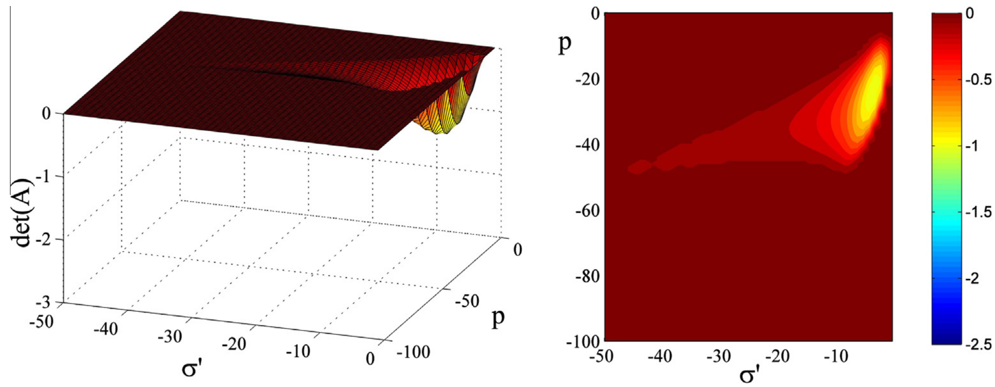

Fig. 9. Discontinuous bifurcation condition in (σ', det(A), p) space for undrained condition assuming plain strain state and local plasticity.

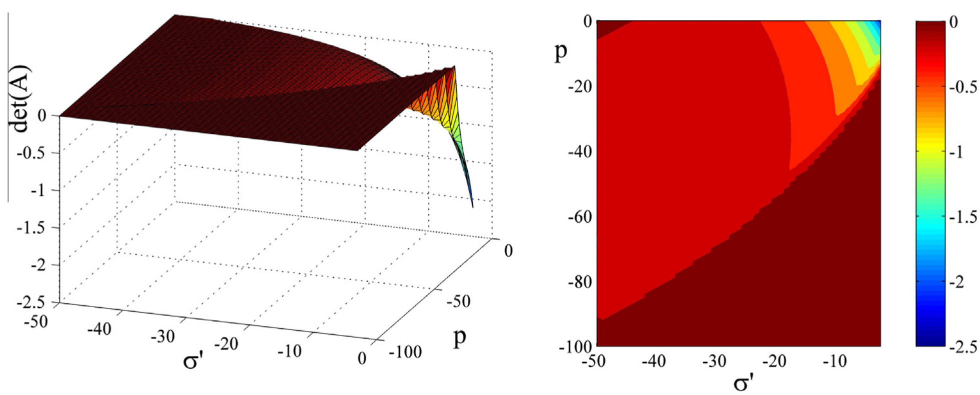

Fig. 10. Discontinuous bifurcation condition in (σ', det(A), p) space for drained condition assuming plain stress state and local plasticity.

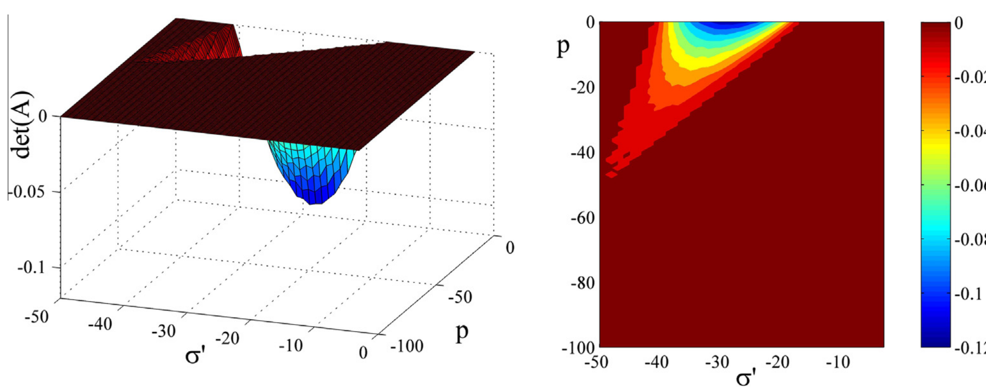

Fig. 11. Discontinuous bifurcation condition in (σ', det(A), p) space for undrained condition assuming plain stress state and local plasticity.

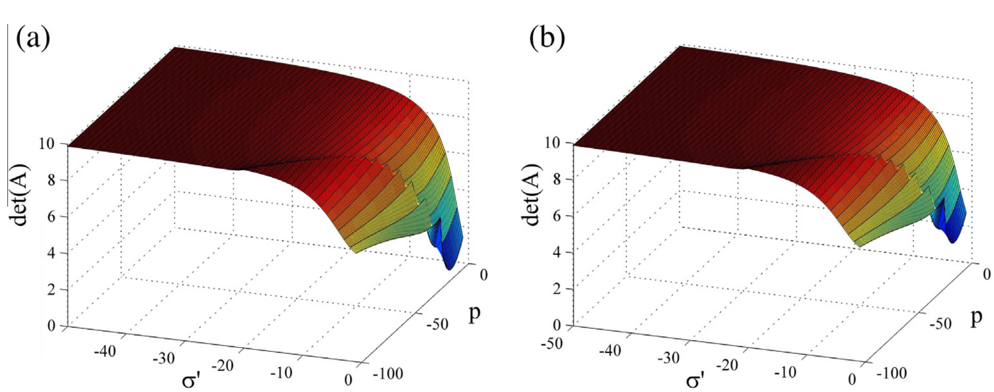

Fig. 12. Discontinuous bifurcation condition in (σ', det(A), p) space assuming plain strain state and gradient-plasticity for: (a) drained condition; (b) undrained condition.

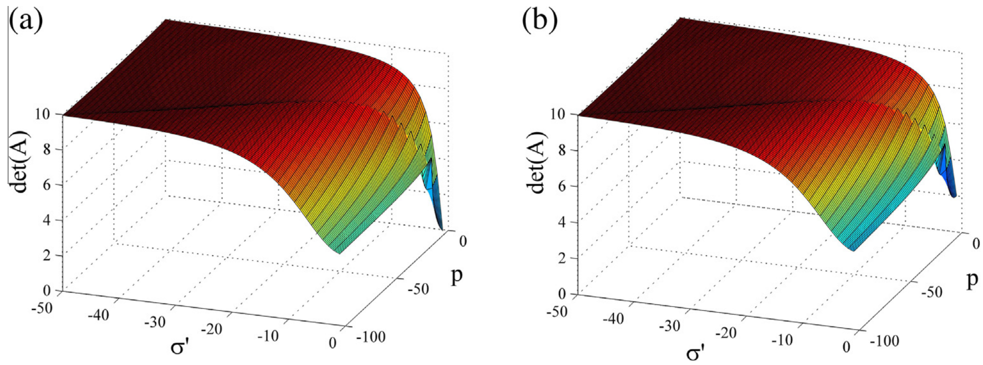

Fig. 13. Discontinuous bifurcation condition in (σ', det(A), p) space assuming plain stress state and gradient-plasticity for: (a) drained condition; (b) undrained condition.

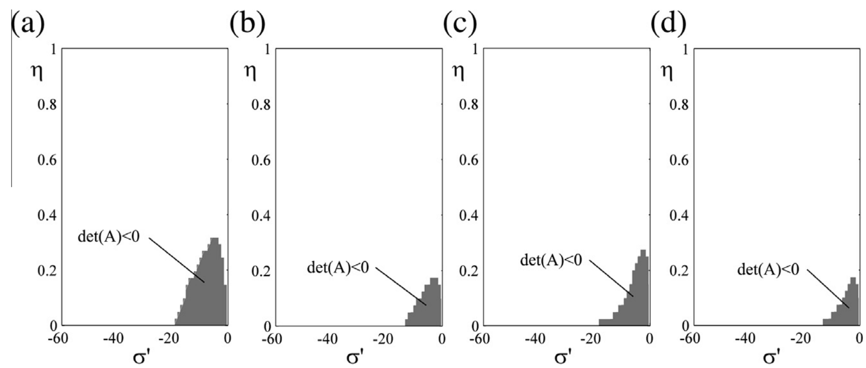

Fig. 14. Influence of non-associativity degree, under plain strain state and: (a) drained condition for local plasticity; (b) undrained condition for local plasticity; (c) drained condition for non-local plasticity; (d) undrained condition for non-local plasticity.

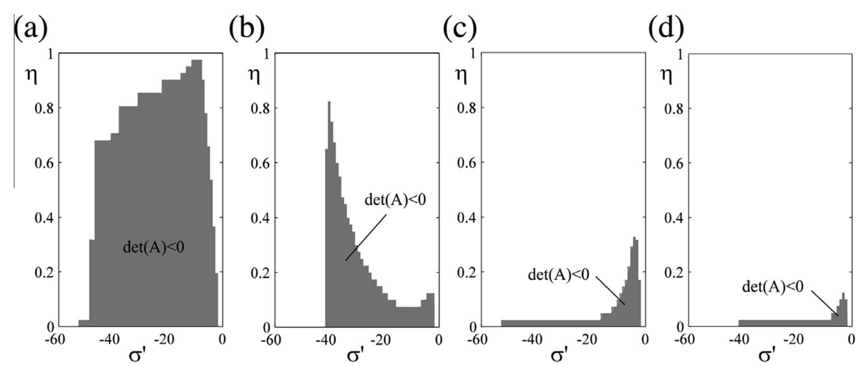

Fig. 15. Influence of non-associativity degree, under plain stress state and: (a) drained condition for local plasticity; (b) undrained condition for local plasticity; (c) drained condition for non-local plasticity; (d) undrained condition for non-local plasticity.

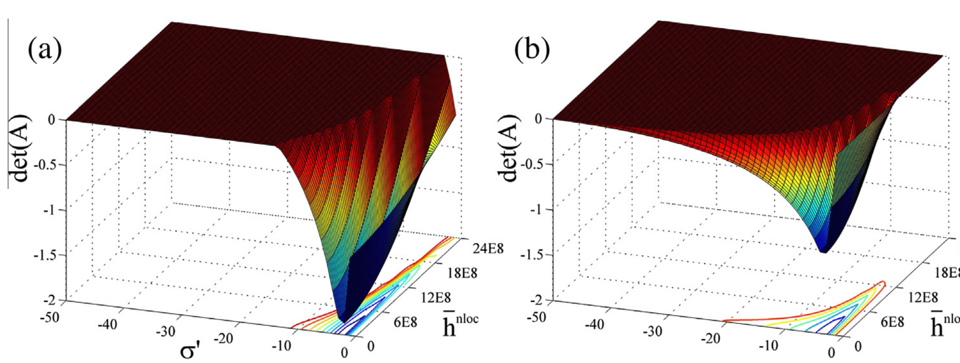

Fig. 16. Limitation of gradient-based poroplasticity formulation for an initial value of the pore pressure equal to −10 kpa, assuming drained condition and: (a) plain strain; (b) plain stress.

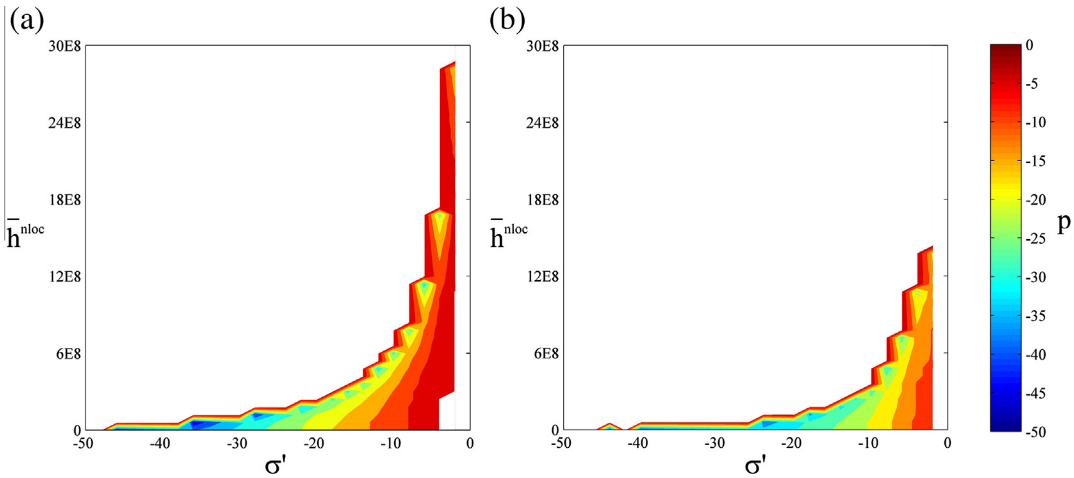

Fig. 17. Limitation of gradient-based poroplasticity formulation for: (a) drained condition; (b) undrained condition, assuming plain strain condition.

demonstrate that the case 2 of Section 5.1 leads to discontinuous bifurcations in the gradient poroplastic theory. As before, the drained condition is more critical than the undrained one.

7. Conclusions

The conditions for localized failure in the form of discontinuous bifurcation were analyzed in the framework of thermodynamically consistent elastoplastic theories for partially saturated porous materials like soils. Local and gradient-based non-local forms of this constitutive theory were considered. A particular form of gradient poroplastic theory was taken into account whereby the state variables are the only ones of non-local character.

The numerical method for the analysis of discontinuous bifurcation consists in the evaluation of the stress domain where the singularity of the localization tensor is fulfilled. In the analytical procedure, the performance of explicit solutions of the critical/minimum hardening modulus corresponding to the first singularity of the localization tensor in the deformation history are evaluated. Also, the localization tensor and the analytical solutions of the minimum hardening modulus for localization were formulated for the local and gradient-based poroplastic constitutive theories particularized for the Cam-clay model, under both drained and undrained hydraulic conditions.

Under consideration of plane strain and plane stress states, the numerical results demonstrate that the hydraulic and stress conditions play a relevant role in the failure performance of local and non-local partially saturated soil materials. Both materials show that drained hydraulic condition are considerably more critical for localization and discontinuous bifurcation than the undrained one. In the local poroplastic material the results show that the failure modes along the maximum strength surface vary from very localized and brittle to diffuse and ductile as the confinement pressure increases. Particularly, under the more critical hydraulic condition (drained case), the region in the stress space associated with localized failure modes covers a sector of much higher confinement in case of plane stress state than in plane strain one.

The gradient-based poroplastic material does not show a real transition point dividing the regions in the stress space characterized with localized and diffuse failure modes, in none of the considered hydraulic and stress conditions. Nevertheless, and due to the particular forms the gradient characteristic lengths of the pore and skeleton phases are defined in the non-local constitutive material, the conditions for discontinuous bifurcation are very closed to be fulfilled in the low confinement regime of the stress space, particularly under drained conditions. This means that under these hydraulic and confinement conditions, and in both plane strain and plane stress states, the considered non-local porous material leads to strong reductions of the failure diffusion, while keeping the well-posedness of the related differential constitutive equations. This is in agreement with the physical reality and demonstrates the capabilities of the constitutive theory to capture quasi-brittle failure modes without losing the strong ellipticity of the involved differential equations.

Finally, a particular case where the regularization capabilities of the gradient-based poroplastic theory in this work is suppressed, was also evaluated. The results demonstrate this deficiency of the non-local theory which is clearly more critical in case of drained hydraulic conditions.

Appendix A. Expressions for the plastic consistency condition

For the sake of clarity last equation is rewritten in compacted form

$$-\dot{\Phi}^{nloc} + \left(\bar{h} + \bar{h}^{nloc}\right)\dot{\lambda} = \dot{\Phi}^{e} - \dot{\Phi} \tag{A.1}$$

where $\dot{\Phi}^e$ is the local loading function, $\bar{h}$ the generalized plastic modulus, $\bar{h}^{nloc}$ the gradient plastic modulus, and $\dot{\Phi}^{nloc}$ the gradient loading function defined as

$$\dot{\Phi}^{nloc} = l_\alpha^2 \partial_{Q_\alpha}\Phi\left\{\partial_{Q_\alpha}\Phi^*\left[H^{nloc}_{\alpha ij}\dot{\lambda}_{,ij} + H^{nloc}_{\alpha ij,j}\dot{\lambda}_{,i}\right] + +2\partial^2_{Q_\alpha Q_\alpha}\Phi^* Q_{\alpha,i}H^{nloc}_{\alpha ij}\dot{\lambda}_{,j}\right\} \tag{A.2}$$

$$\bar{h}^{nloc} = -l_\alpha^2\partial_{Q_\alpha}\Phi\left\{\partial^2_{Q_\alpha Q_\alpha}\Phi^*\left[H^{nloc}_{\alpha ij}Q_{\alpha,ij} + H^{nloc}_{\alpha ij,j}Q_{\alpha,i}\right] + +\partial^3_{Q_\alpha Q_\alpha Q_\alpha}\Phi^* Q_{\alpha,i}H^{nloc}_{\alpha ij}Q_{\alpha,j}\right\} \tag{A.3}$$

Both, the local yield function and the generalized plastic modulus can be decomposed into the components $(\dot{\Phi}^e_s, h_s)$ and $(\dot{\Phi}^e_p$ and $h_p)$ related to the soil skeleton and to the porous, respectively. This decomposition is valid for undrained and drained conditions.

$$\dot{\Phi}^e = \dot{\Phi}^e_s + \dot{\Phi}^e_p \tag{A.4}$$

$$\bar{h} = h_s + h_p + \bar{H} \tag{A.5}$$

with

$$\bar{H} = H^{loc}_\alpha \partial_{Q_\alpha}\Phi\partial_{Q_\alpha}\Phi^* \tag{A.6}$$

where, for drained condition, it can be obtained

$$\dot{\Phi}_s^{e,d} = \partial_{\sigma_{ij}} \Phi C^0_{ijkl} \dot{\varepsilon}_{kl} \tag{A.7}$$

$$\dot{\Phi}_p^{e,d} = \left(\partial_p \Phi - \partial_{\sigma_{ij}} \Phi B_{ij} \right) \dot{p} \tag{A.8}$$

$$h_s^d = \partial_{\sigma_{ij}} \Phi C^0_{ijkl} \partial_{\sigma_{kl}} \Phi^* \tag{A.9}$$

$$h_p^d = 0 \tag{A.10}$$

while for undrained condition

$$\dot{\Phi}_s^{e,u} = \partial_{\sigma_{ij}} \Phi C_{ijkl} \dot{\varepsilon}_{kl} - \mathrm{M} \partial_p \Phi B_{ij} \dot{\varepsilon}_{ij} \tag{A.11}$$

$$\dot{\Phi}_p^{e,u} = \frac{\dot{m}}{\rho_0^{fl}} \left(\mathrm{M} \partial_p \Phi - \partial_{\sigma_{ij}} \Phi B_{ij} \right) \tag{A.12}$$

$$h_s^u = \partial_{\sigma_{ij}} \Phi C_{ijkl} \partial_{\sigma_{kl}} \Phi^* \tag{A.13}$$

$$h_p^u = -\mathrm{M} \left(\partial_{\sigma_{ij}} \Phi B_{ij} \partial_p \Phi^* + \partial_p \Phi B_{ij} \partial_{\sigma_{ij}} \Phi^* - \partial_p \Phi \partial_p \Phi^* \right) \tag{A.14}$$

Appendix B. Constitutive relationship for gradient-based poroplasticity

The gradient-plasticity constitutive relationship of Eq. (15) with drained conditions are

$$E^{ep,sd}_{ijkl} = C^0_{ijkl} - \frac{C^0_{ijmn} \partial_{\sigma_{mn}} \Phi^* \partial_{\sigma_{pq}} \Phi C^0_{pqkl}}{\bar{h}} \tag{B.1}$$

$$E^{ep,pd}_{ij} = -B_{ij} - \frac{C^0_{ijkl} \partial_{\sigma_{kl}} \Phi^* \left(\partial_p \Phi - \partial_{\sigma_{mn}} \Phi B_{mn} \right)}{\bar{h}} \dot{p} \tag{B.2}$$

$$E^{g,spd}_{ij} = \frac{C^0_{ijkl} \partial_{\sigma_{kl}} \Phi^*}{\bar{h}} \tag{B.3}$$

$$\dot{f}^g = l^2_\alpha \partial_{Q_\alpha} \Phi \partial_{Q_\alpha} \Phi^* H^{nloc}_{\alpha\, ij} \dot{\lambda}_{,ij} \tag{B.4}$$

In the same way, the gradient-plasticity constitutive relationship of Eq. (16) with undrained conditions are presented here as

$$E^{ep,su}_{ijkl} = C_{ijkl} - \frac{C_{ijmn} \partial_{\sigma_{mn}} \Phi^* \partial_{\sigma_{pq}} \Phi C_{pqkl}}{\bar{h}} - \mathrm{M}^2 \frac{\partial_p \Phi^* B_{ij} B_{kl} \partial_p \Phi}{\bar{h}} + \mathrm{M} \left(\frac{C_{ijmn} \partial_{\sigma_{mn}} \Phi^* B_{kl} \partial_p \Phi}{\bar{h}} + \frac{\partial_p \Phi^* B_{ij} C_{mnkl} \partial_{\sigma_{mn}} \Phi}{\bar{h}} \right) \tag{B.5}$$

$$E^{ep,pu}_{ij} = -\mathrm{M} \left(B_{ij} - \frac{\partial_p \Phi^* B_{ij} \left(\mathrm{M} \partial_p \Phi - \partial_{\sigma_{mn}} \Phi B_{mn} \right)}{\bar{h}} \right) - \frac{C_{ijkl} \partial_{\sigma_{kl}} \Phi^* \left(\mathrm{M} \partial_p \Phi - \partial_{\sigma_{mn}} \Phi B_{mn} \right)}{\bar{h}} \tag{B.6}$$

$$E^{g,spu}_{ij} = \frac{C_{ijkl} \partial_{\sigma_{kl}} \Phi^* - \mathrm{M} B_{ij} \partial_p \Phi^*}{\bar{h}} \tag{B.7}$$

$$\dot{f}^g = l^2_\alpha \partial_{Q_\alpha} \Phi \partial_{Q_\alpha} \Phi^* H^{nloc}_{\alpha\, ij} \dot{\lambda}_{,ij} \tag{B.8}$$

References

Abellan, M.-A., de Borst, R., 2006. Wave propagation and localisation in a softening two-phase medium. Comput. Methods Appl. Mech. 195, 5011–5019.
Al Hattamleh, O., Muhunthan, B., Zbib, H.M., 2004. Gradient plasticity modelling of strain localization in granular materials. Int. J. Numer. Anal. Methods 28, 465–481.
Alonso, E.E., Gens, A., Josa, A., 1990. A constitutive model for partially saturated soils. Geotechnique 40 (3), 405–430.
Benallal, A., Comi, C., 2002. Material instabilities in inelastic saturated porous media under dynamic loadings. Int. J. Solids Struct. 39 (13–14), 3693–3716.
Bolzon, G., Schrefler, B., Zienkiewicz, O., 1996. Elastoplastic soil constitutive laws generalized to partially saturated states. Geotechnique 46 (2), 279–289.
Borja, R.I., 2004. Cam-Clay plasticity. Part V: A mathematical framework for three-phase deformation and strain localization analyses of partially saturated porous media. Comput. Methods Appl. Mech. 193, 5301–5338.
Cetin, H., Gökoĝlu, A., 2013. Soil structure changes during drained and undrained triaxial shear of a clayey soil. Soils Found. 53 (5), 628–638.
Coussy, O., 1995. Mechanics of Porous Continua. John Wiley & Sons.
Ehlers, W., Graf, T., Ammann, M., 2004. Deformation and localization analysis of partially saturated soil. Comput. Methods Appl. Mech. 193 (27–29), 2885–2910.
Etse, G., Caggiano, A., Vrech, S., 2012. Multiscale failure analysis of fiber reinforced concrete based on a discrete crack model. Int. J. Fract. 178 (1–2), 131–146.
Hadamard, J., 1903. Propagation des Ondes et Les Equations d'Hydrodynamique. Chelsea, New York (reprinted 1949).
Kristensson, O., Ahadi, A., 2005. Numerical study of localization in soil systems. Comput. Geotech. 32 (8), 600–612.
Liebe, T., Steinmann, P., Benallal, A., 2001. Theoretical and computational aspects of a thermodynamically consistent framework for geometrically linear gradient damage. Comput. Methods Appl. Mech. 190, 6555–6576.
Liu, X., Scarpas, A., 2005. Numerical modeling of the influence of water suction on the formation of strain localization in saturated sand. CMES – Comput. Model Eng. 9 (1), 57–74.
Mroginski, J.L., Etse, G., 2013. A finite element formulation of gradient-based plasticity for porous media with C1 interpolation of internal variables. Comput. Geotech. 49, 7–17.
Mroginski, J.L., Etse, G., Vrech, S.M., 2011. A thermodynamical gradient theory for deformation and strain localization of porous media. Int. J. Plast. 27, 620–634.
Ottosen, N.S., Runesson, K., 1991. Properties of discontinuous bifurcation solutions in elasto-plasticity. Int. J. Solids Struct. 27 (4), 401–421.
Pedroso, D.M., Farias, M.M., 2011. Extended Barcelona basic model for unsaturated soils under cyclic loadings. Comput. Geotech. 38 (5), 731–740.
Perić, D., 1990. Localized Deformation and Failure Analysis of Pressure Sensitive Granular Materials (Ph.D. thesis). University of Colorado, CEAE Dept., Boulder.
Perić, D., Rasheed, H.A., 2007. Localized failure of fibre-reinforced elastic-plastic materials subjected to plane strain loading. Int. J. Numer. Anal. Methods 31 (7), 893–916.
Roscoe, K., Burland, J., 1968. On the generalized stress–strain behaviour of wet clay. In: Heyman, J., Leckie, F.A. (Eds.), Engineering Plasticity. Cambridge University Press.
Runesson, K., Ottosen, N.S., Dunja, P., 1991. Discontinuous bifurcations of elastic–plastic solutions at plane stress and plane strain. Int. J. Plast. 7 (1–2), 99–121.
Runesson, K., Perić, D., Sture, S., 1996. Effect of pore fluid compressibility on localization in elastic–plastic porous solids under undrained conditions. Int. J. Solids Struct. 33 (10), 1501–1518.
Sabatini, P.J., Finno, R.J., 1996. Effect of consolidation on strain localization of soft clays. Comput. Geotech. 18 (4), 311–339.
Sawicki, A., Świdziński, W., 2010. Modelling the pre-failure instabilities of sand. Comput. Geotech. 37 (6), 781–788.
Schiava, R., Etse, G., 2006. Constitutive modelling and discontinuous bifurcation assessment in unsaturated soils. J. Appl. Mech. 73 (6), 1039–1044.
Schrefler, B.A., Zhang, H.W., Sanavia, L., 2006. Interaction between different internal length scales in strain localization analysis of fully and partially saturated porous media – the 1-D case. Int. J. Numer. Anal. Methods 30 (1), 45–70.
Sulem, J., 2010. Bifurcation theory and localization phenomena. Eur. J. Environ. Civil Eng. 14 (1–10), 989–1009.
Svedberg, T., Runesson, K., 1997. A thermodynamically consistent theory of gradient-regularized plasticity coupled to Damage. Int. J. Plast. 13 (6–7), 669–696.
Tsagrakis, I., Konstantinidis, A., Aifantis, E., 2003. Strain gradient and wavelet interpretation of size effects in yield and strength. Mech. Mater. 35, 733–745.
Vardoulakis, I., 1996. Deformation of water-saturated sand. I: Uniform undrained deformation and shear banding. Geotechnique 46 (3), 441–456.
Vrech, S., Etse, G., 2006. Geometrical localization analysis of gradient-dependent parabolic Drucker–Prager elatoplasticity. Int. J. Plast. 22 (5), 943–964.
Vrech, S.M., Etse, G., 2009. Gradient and fracture energy-based plasticity theory for quasi-brittle materials like concrete. Comput. Methods Appl. Mech. 199 (1–4), 136–147.
Vrech, S.M., Etse, G., 2012. Discontinuous bifurcation analysis in fracture energy-based gradient plasticity for concrete. Int. J. Solids Struct. 49 (10), 1294–1303.
Zhang, H.W., Schrefler, B.A., 2001. Uniqueness and localization analysis of elastic–plastic saturated porous media. Int. J. Numer. Anal. Methods 25 (1), 29–48.
Zhang, Y.Q., Hao, H., Yu, M.H., 2002. Effect of porosity on the properties of strain localization in porous media under undrained conditions. Int. J. Solids Struct. 39 (7), 1817–1831.
Zhang, H.W., Zhou, L., Schrefler, B.A., 2005. Material instabilities of anisotropic saturated multiphase porous media. Eur. J. Mech. A-Solid 24 (5), 713–727.
Zhen, W., Sun, D., Chen, Y., 2010. Analytical solution and numerical simulation of shear bands along different stress paths in three-dimensional stress state. Geotech. Sp. 200, 192–197.